Title

Peripheral neuropathy induced by microtubule-targeted chemotherapies: insights into acute injury and long-term recovery

Journal

Cancer Research, 78(3)

ISSN

0008-5472

Authors

Wozniak, Krystyna M
Vornov, James J
Wu, Ying
et al.

Publication Date

2018-02-01

DOI

10.1158/0008-5472.can-17-1467

Peer reviewed

HHS Public Access

Author manuscript

Cancer Res. Author manuscript; available in PMC 2019 February 01.

Published in final edited form as:

Cancer Res. 2018 February 01; 78(3): 817–829. doi:10.1158/0008-5472.CAN-17-1467.

Peripheral neuropathy induced by microtubule-targeted chemotherapies: *insights into acute injury and long-term recovery*

Krystyna M. Wozniak[1], **James J. Vornov**[2], **Ying Wu**[1], **Ying Liu**[3], **Valentina A. Carozzi**[4], **Virginia Rodriguez-Menendez**[4], **Elisa Ballarini**[4], **Paola Alberti**[4], **Eleonora Pozzi**[4], **Sara Semperboni**[4], **Brett M. Cook**[5,6], **Bruce A. Littlefield**[7], **Kenichi Nomoto**[7], **Krista Condon**[7], **Sean Eckley**[7], **Christopher DesJardins**[8], **Leslie Wilson**[5,6,9], **Mary A. Jordan**[5,9], **Stuart C. Feinstein**[5,9], **Guido Cavaletti**[4], **Michael Polydefkis**[3], and **Barbara S. Slusher**[10]

[1]Johns Hopkins Drug Discovery, Johns Hopkins School of Medicine, Baltimore, MD

[2]Medpace, Cincinnati, OH

[3]Department of Neurology and the Cutaneous Nerve Laboratory, School of Medicine and Surgery, University of Milano-Bicocca, Monza, Italy

[4]Experimental Neurology Unit and PhD program in Neuroscience, School of Medicine and Surgery, University of Milano-Bicocca, Monza, Italy

[5]Neurosci Research Institute, University of California, Santa Barbara, CA

[6]Biomolecular Science and Engineering Program, University of California, Santa Barbara, CA

[7]Eisai Inc., Andover, MA

[8]Waters Corporation, Milford, MA

[9]Department of Molecular Cellular and Developmental Biology, University of California, Santa Barbara, CA

[10]Johns Hopkins Drug Discovery and Departments of Neurology, Psychiatry, Neuroscience, Medicine and Oncology, Johns Hopkins School of Medicine, Baltimore, MD

Abstract

Chemotherapy-induced peripheral neuropathy (CIPN) is a major cause of disability in cancer survivors. CIPN investigations in preclinical model systems have focused on either behaviors or acute changes in nerve conduction velocity (NCV) and amplitude, but greater understanding of the underlying nature of axonal injury and its long-term processes is needed as cancer patients live longer. In this study, we used multiple independent endpoints to systematically characterize CIPN recovery in mice exposed to the anti-tubulin cancer drugs eribulin (ERIB), ixabepilone (IXA),

Corresponding Author: Barbara S Slusher, Ph.D., Professor, Neurology (*primary*), Psychiatry, Neuroscience, Medicine and Oncology, Johns Hopkins School of Medicine, Rangos Suite 277, 855 North Wolfe Street, Baltimore, MD 21205, 410-614-0662 (office); 410-960-6162 (cell); 410-614-0659 (fax); bslusher@jhmi.edu.

Conflicts of Interest: BAL, KN, KC, SE, and CD are, or were at the time of the studies reported here, full-time employees of Eisai Inc., which manufactures and markets eribulin as its clinical formulation, Halaven®. Other authors report no conflicts of interest.

paclitaxel (PACLI) or vinorelbine (VINO) at maximal tolerated doses. All of the drugs ablated intra-epidermal nerve fibers and produced axonopathy, with a secondary disruption in myelin structure within two weeks of drug administration. Additionally, all of the drugs reduced sensory NCV and amplitude, with greater deficits after PACLI and lesser deficits after IXA. These effects correlated with degeneration in dorsal root ganglia (DRG) and sciatic nerve and abundance of Schwann cells. While most injuries were fully reversible after 3–6 months after administration of ERIB, VINO, and IXA, we observed delayed recovery after PACLI that produced a more severe, pervasive and prolonged neurotoxicity. Compared to other agents, PACLI also displayed a unique prolonged exposure in sciatic nerve and DRG. The most sensitive indicator of toxicity was axonopathy and secondary myelin changes accompanied by a reduction in intra-epidermal nerve fiber density. Taken together, our findings suggest that intra-epidermal nerve fiber density and changes in NCV and amplitude might provide measures of axonal injury to guide clinical practice.

Keywords

Chemotherapy; neuropathy; microtubule inhibitors; intra-epidermal nerve fiber density; nerve conduction; eribulin; paclitaxel; ixabepilone; vinorelbine

INTRODUCTION

Chemotherapy-induced peripheral neuropathy (CIPN) is a prominent side effect of chemotherapies that target microtubules (1–4). CIPN can lead to dose reduction associated with poorer survival (5) and can be disabling for patients (1,6,7). While CIPN has been frequently observed in cancer survivors, often outlasting the course of chemotherapy (4,8,9), the severity of CIPN and time course of recovery following treatment with anti-microtubule agents is not well studied. Most clinical investigations focus on the incidence and severity of neuropathy during treatment. However, in clinical practice, patients are often treated with combinations of drugs that are individually known to cause CIPN and receive sequential treatment for recurrence with additional CIPN-inducing drugs. Thus, while different chemotherapeutic regimens vary clinically in the frequency and severity of resultant CIPN, little is known about the relative reversibility from individual agents and the vulnerability of nerves to long-term injury.

Animal models have proven useful to investigate how chemotherapies differ in their patterns of producing neuropathy, axonopathy and myelinopathy (10–13). For example, we have previously reported that paclitaxel (PACLI) and ixabepilone (IXA) produce more severe nerve conduction and morphology changes in mice compared to ERIB at their respective maximal tolerated doses (MTD) (14). We have also provided evidence that microtubule agents can accumulate and persist in nerves, although this does not correlate with the severity of neuropathy as assessed by nerve conduction deficits observed for weeks following exposure (15). While changes in nervous tissue morphology (16), mitochondrial structure (17,18) and distal site skin innervation (19,20) have been described, there have been no systematic long term comparisons of recovery of different peripheral nerve subsets from axonal and DRG injury. To understand more fully the underlying nature of nerve injury and its recovery over time we have directly compared the severity and extent of peripheral

nervous system recovery in mice for up to six months after exposure to maximally tolerated doses of four antimicrotubule chemotherapies: eribulin (ERIB), ixabepilone (IXA), paclitaxel (PACLI) and vinorelbine (VINO). In addition, we investigated microtubule biochemistry, Schwann cell actions and long-term drug disposition relative to the extent to which damage persists. This neuropathy recovery study may help better understand the long-term effects of ERIB, IXA, PACLI and VINO on the peripheral nervous system, which may ultimately serve to guide their clinical use.

METHODS

Experimental Design

The overall experimental design including the schedule of drug administration and timing of assessments is shown schematically in Figure 1. Female BALB/c mice (7–8 weeks old) were obtained from Envigo (Indianapolis, IN) and maintained with free access to water and a standardized synthetic diet (Envigo Teklad Global Rodent Diet). Animal housing and procedure room temperature and humidity were maintained at 20 ± 2°C and 55 ± 10% respectively. Artificial lighting provided a 12h light/12h dark cycle (light 7am–7pm). Experimental protocols were approved by the Institutional Animal Care and Use Committee of John Hopkins University and adhered to all applicable institutional and governmental guidelines for humane treatment set forth in the Guide for the Care and Use of Laboratory Animals (Office of Laboratory Animal Welfare, National Institutes of Health). Mice were treated with a previously determined 6-dose MTD regimen administered intravenously, dosing every other day for 2 weeks with a 2 day drug-free gap between weekly cycles (14). MTD was determined as the maximal dose at which no more than one per group of ten animals died spontaneously within a 2-week period after cessation of dosing, or at which no more than one mouse in the group required euthanasia due to >20% weight loss or overt clinical signs of distress including inability to eat or drink. The 6-dose intravenous MTD regimen was determined to be 1.2 mg/kg for ERIB, 2 mg/kg for IXA, 30 mg/kg for PACLI and 11 mg/kg for VINO.

Drugs and Formulations

Eribulin mesylate (synthesized and provided by Eisai Inc. and stored desiccated at −80°C in the dark) was dissolved in 100% anhydrous DMSO (Sigma-Aldrich, St. Louis, MO) to produce a 10 mg/mL stock solution, which was separated into aliquots and stored at –80°C. Each administration day an aliquot of the stock solution was thawed and diluted with saline to a final concentration of 0.12 mg/mL in 2.5% DMSO/97.5% saline and administered in a 10 mL/kg volume. PACLI (purchased from LC Laboratories, Woburn, MA and stored at −20°C in the dark) was dissolved in ethanol (100%) at 10% of final volume. An equal volume of cremophor (10% of final volume) was then added and the mixture re-vortexed for about 10 min. Immediately prior to injection, ice cold saline was added to final volume (as 80% of final) and the solution was maintained on ice during dosing. Dosing solutions of 3 mg/mL were made fresh on each dosing day and administered in a 10 mL/kg volume. IXA (Ixempra, Bristol-Myers Squibb, N.J.) was prepared according to the package insert. The formulated IXA stock solution (2 mg/mL) was immediately aliquoted and stored at –80°C until use. On each experimental day, an aliquot of the stock solution was diluted by adding

50% ethanol/50% cremophor with subsequent vortexing to yield a resultant solution that was 5 times the required dosing concentration. Four volumes of PBS were added, while vortexing, to achieve a final dosing concentration of 10 mL/kg. VINO (United States Pharmacopeia, Rockville, MD) was prepared fresh each dosing day by dissolving powder in sterile normal saline and formulating at 1.1 mg/mL for dosing at 10 mL/kg.

Nerve Conduction Velocity and Amplitude

Electrophysiological measurements were performed as previously described (14,21). In brief, baseline caudal and digital nerve conduction velocity (NCV) and amplitude were measured in all mice the week prior to dosing. Mice were anesthetized with 2% isoflurane (by inhalation, for induction and maintenance) and placed on a heating pad with rectal temperature maintained between 37.0 – 40.0°C. Platinum subdermal needle electrodes (Grass Technologies, West Warwick, RI) were used for stimulating and recording. Caudal NCV was recorded from electrodes placed in a bipolar configuration at the base of the tail (at the hair line); the stimulating cathode being positioned 35 mm further distal. Digital NCV was recorded using stimulation at the base of the second toe and recording at the level of the lateral malleolus. Amplitudes were measured as the baseline to peak neural response. Each nerve segment stimulation was repeated at least 3 times, up to a maximum of 6 times, with increasing voltage until the maximal response was achieved, using AcqKnowledge software version 3.7.3 (BIOPAC Systems Inc.). Mice (10 per group) were randomly assigned into a vehicle, eribulin, ixabepilone, paclitaxel or vinorelbine treatment group (* *VINO group was repeated twice as detailed below in the RESULTS section).* A common cremophor-based vehicle group was used for comparison with the PACLI and IXA treatment groups in order to reduce mouse usage numbers, with individual vehicle groups for ERIB and VINO. Following MTD dosing as described above, mice were again tested for NCV/amplitude at 24 hours, 7 days, and 14 days and at 1 month, 2 months, 3 months and 6 months following the last dose. Statistical analysis of data was made by Students-t test using Prism Graphpad software Version 4.03, with significance being defined at $p \leq 0.05$.

Intra-epidermal Nerve Fiber Density

Mice were euthanized with carbon dioxide and footpads were removed from three mice per time point and intra-epidermal nerve fiber densities were quantitated as previously described (22). In brief, hind limbs were transected at the calcaneus bone and placed in Zamboni's fixative for 48 hours after which they were washed with phosphate buffer and placed in cryoprotectant (30% glycerol) solution. Tissue blocks were cut by freezing microtome at 50 μm intervals and immunohistochemical staining was performed using a standard chromogen technique with rabbit anti-PGP 9.5 (AbD Serotec, a Bio-Rad Company, Kidlington, UK). Four sections were selected for staining from a total of 10–12 sections at 100 μm intervals from a tissue block that contained footpads 3 and 4 in order to ensure a systematic sampling of the footpad. Sections were incubated overnight at room temperature with primary antibody at 1:6000 in 96 well tissue culture plates on a horizontal tabletop shaker at 50 rolls per minute. The following day, sections were washed in phosphate buffer 2–3 times and incubated with biotinylated goat anti-rabbit Ab (Vector Labs, Burlingame, CA) for 2–3 h. Bound immunoglobulin was visualized by the ABC kit (Vector labs, Burlingame, CA). Individual PGP 9.5 positive intra-epidermal nerve fibers crossing the dermal-epidermal

junction were counted by manual inspection. IENFD was calculated by dividing the number of counted fibers by the length of epidermis and expressed as fibers/mm. Statistical analysis of data was performed using Students t-test analysis versus vehicle-treated mice.

Drug Exposure

In the same mice, pharmacokinetic (PK) studies were performed to determine the plasma, DRG and SN exposure of the four drugs after the MTD administrations. Mice were euthanized with CO_2 and plasma and tissues were taken at 24 hour, 7 days, 14 days, 1 month, 2 months, 3 months and 6 months following the last dose (n=3 mice per group and time point). Blood was removed via cardiac puncture and plasma was derived from whole blood by centrifugation at 3000 RPM at 4°C in plasma separator tubes for 10 min. SN and DRG were removed and pooled and homogenized with three times their respective weights of mouse plasma using a MiniBead Beater-96. All samples were stored at −80°C until analysis. Samples were analyzed for ERIB, IXA, PACLI and VINO using reverse phase chromatography on a LC-MS/MS (API-4000 with a Shimadzu autosampler) using methods based on procedures previously described (23–25). The lower limits of quantifications for ERIB, IXA, PACLI and VINO respectively, were 0.5, 5, 1 and 2 ng/mL in plasma, 6.25, 125, 25 and 10 ng/g in DRG, and 5, 100, 20 and 8 ng/g in SN.

Neuropathological Analyses

For neuropathological analyses, three mice from each treatment group at the 2 week, 3 month and 6 month time points underwent total body perfusion with phosphate buffer solution containing 2% glutaraldehyde and 4% paraformaldehyde while under deep anesthesia. L4–L5 DRG and both sciatic nerves at mid-thigh were dissected from the mice without stretching. For morphological evaluation, specimens were fixed by immersion in 3% glutaraldehyde (left sciatic nerves) or 2% glutaraldehyde/4% paraformaldehyde (DRG) in 0.12 M phosphate buffer solution, post-fixed in OsO_4, epoxy resin embedded and used for light microscopy and morphometric analysis. For immunofluorescence/antibody staining, sciatic nerves were post-fixed in 4% para-formaldehyde in 0.12 M phosphate buffer solution.

Morphological and Morphometric Evaluation of DRG and Sciatic Nerve

Semi-thin 1-μm sections of sciatic nerves and DRG were prepared, stained with toluidine blue and examined with a Nikon Eclipse E200 light microscope (Leica Microsystems GmbH, Wetzlar, Germany) as previously described (26). Representative images were captured with a light microscope-incorporated camera (Leica DFC 280 Wetzlar, Germany). Morphometric analysis of sciatic nerves was performed at a magnification of 60X using a QWin automatic image analyzer (Leica Microsystems GmbH, Wetzlar, Germany). In randomly selected fields of the nerve sections (at 5 mm from the proximal stump), all myelinated fibers evaluable in the analyzed space were counted and the internal (axonal) and external (total) diameters of myelinated fibers were measured on at least 500 myelinated fibers/nerve. The histograms of g-ratio (axonal diameter/whole fiber diameter as a measure of myelination degree in each fiber) distribution were generated. The same blinded observer performed all the morphometric determinations according to earlier published methods (26,27)

For DRG morphometrics, serial 1-μm sections, spaced at 25 μm intervals, were collected and stained as described above. Images were captured with a light microscope-incorporated camera (Leica DFC 280 Wetzlar, Germany) at an original magnification of 20x. The somatic, nuclear and nucleolar size of at least 200 DRG neurons/animal were manually measured and analyzed with a computer-assisted image analyzer (Image J software, US National Institutes of Health). The same blinded observer performed all the morphometric measurements as described earlier (26,28). Statistical analysis was performed using Student's t test.

Sciatic Nerve Immunohistochemistry, Imaging and Analysis

Fixed whole sciatic nerves were processed as described previously (29). Briefly, nerves were embedded in 10% agarose and Vibratome cross-sectioned at 100 μm steps and stored in 1X PBS containing 0.01% sodium azide at 4°C until immunostaining. Individual sections were stained with antibodies to acetylated α-tubulin (K40, Cell Signaling #5335, 1:800 dilution), GFAP (Abcam #7260, 1:200 dilution), or S100B (Abcam Ab11178, 1:500 dilution). All sections were also stained with anti-phosphoneurofilament (Covance SMI-31R 1:2000 dilution) and anti-myelin basic protein (Millipore AB9348, 1:100 dilution) as internal controls and to identify regions of interest (axons and myelin sheaths, respectively). Sections were blocked in PBT blocking agent overnight at 4°C [PBS (1.37 M NaCl, 27 mM KCl, 100 mM Na2HPO4, 18 mM KH2PO4), 0.1% TritonX-100, 1% BSA, 1% donkey serum]. Sections were then incubated free-floating at 4°C with primary antibodies for seven days followed by incubation with fluorescently-labelled secondary antibodies for two days. Sections were mounted using ProLong Gold mounting media with DAPI (Life Technologies P36935). Each slide was prepared containing one section from each of the four treatments and one section from each of the corresponding vehicle controls, all stained simultaneously with the same antibody solution. Z-stacks of the first 20 μm of each section were collected at 0.5 μm steps using an Olympus Fluoview 1000 Spectral confocal system equipped an Olympus PLANAPOSC 60x (1.40 NA) high refractive index oil immersion objective excited by 405, 488, 559 and 635 nm laser lines, and collected by PMT detectors. Images from each slide were imported into Imaris (Version 7.5.2, Bitplane, Zurich, Switzerland) and rendered into three dimensional maximum intensity z-stack projections for analysis (see Supplementary Figure S1 and Supplementary Methods for additional procedures).

DATA COLLECTION AND ANALYSIS

In all cases, mice were randomly assigned into treatment groups with the exception of the second VINO group which was repeated due to early deaths (see methods/results for details). Sample sizes estimations were based on similar experiments performed previously by our group. When acquiring data, experimenters were blind to specific group assignments. All results are presented as mean ± standard error of mean (SEM). Prism Graphpad software Version 4.03 was used for statistical analysis. All analyses of changes in nerve conduction velocity and amplitude, sciatic nerve morphology, morphometry, microtubule biochemistry, and IENFD data were performed using a Student's t test comparing to vehicle-treated mice at the same time points (*$p<0.05$, **$p<0.01$, ***$p<0.001$).

RESULTS

Nerve Conduction and Amplitude Effects

The effect of the MTD dosing regimen on NCV and amplitude measurements varied. Of the four drugs tested, PACLI effects were most severe, significantly slowing both caudal and digital NCV and reducing caudal and digital nerve amplitude at all time points from 24 hours through 6 months of recovery (Figures 2A–H and 3A–H). The largest deficit was observed 1–2 weeks after dosing, with larger effects seen on amplitude compared to NCV (Figures 2A and 2B). IXA and ERIB produced less severe, although still significant, deficits in NCV (Figures 2C and 2E). Small, but significant reductions in caudal amplitude were also observed after dosing with IXA and ERIB (Figures 2D and 2F), while only IXA produced a significant effect on digital amplitude (Figures 3B, 3D, 3F and 3H). Interestingly, the amplitude effects, while small, tended to be delayed showing maximal deficit at 1–2 months post dosing for IXA and ERIB, respectively.

Recording from VINO-treated mice was complicated by an unexpectedly high death rate (90%) just before completing 2 months of recovery. To investigate this further, a second cohort was treated similarly and again a high death rate (80%) occurred. The facility veterinarian conducted autopsies on several of the mice, and deemed the deaths to be non-specific and likely due to repeated anesthesia for nerve conduction measurement, since VINO-treated mice in the pharmacokinetic and morphology groups all survived the 6 months recovery without incidence. Interestingly, this apparent delayed and lethal association between VINO treatment and repeated anesthesia was not seen with the other microtubule-targeting drugs. Accordingly, nerve conduction measurements in VINO-treated mice were only followed for up to 4 weeks after dosing. VINO-treated mice had a significant decrease in caudal velocity at 24 hours and a decrease in digital velocity at 2 weeks post dose. Neither digital nor caudal amplitude were significantly affected by VINO treatment (Figures 2H and 3H).

Intra-epidermal Nerve Fiber Density

As shown in Figure 4, all four antitubulin agents produced a reversible decrease in footpad epidermal nerve fiber density that generally peaked 2 weeks after the end of dosing. The loss was largest and of longest duration after PACLI, with recovery requiring a full 6 months (Figure 4A). The effects of VINO and ERIB were similar having a rapid onset and recovery after 4 weeks. The IXA-induced epidermal nerve fiber density decrease was about the same magnitude, but developed more slowly, than that seen with the other agents. Representative photomicrographs of IENFD from PACLI and Vehicle treated mice are shown in Figure 4B.

Drug Exposure

All four chemotherapies administered were cleared from plasma rapidly with only PACLI and VINO treated mice showing quantifiable levels 24 hours after cessation of dosing (of 4.68 and 5.56 ng/mL respectively; Table 1). In contrast, each of the four chemotherapies showed quantifiable levels in DRG and SN for several days after cessation of dosing. PACLI had the longest exposure duration with quantifiable levels in DRG and SN remaining up to 2 months after completion of dosing. By comparison, ERIB and VINO treated mice showed

quantifiable levels in SN and DRG for only 7 to 14 days post-dosing. IXA treated mice had quantifiable levels in DRG only through 7 days post-dosing and no detectible drug in SN at any time point.

DRG and Sciatic Nerve Morphology/Morphometry

Of the four chemotherapies evaluated, only PACLI and IXA produced DRG and sciatic nerve morphology changes (Figure 5A–L, Supplementary Figures 2S A–L and 3S A–L). Following PACLI, dark inclusions were present in DRG sensory neurons at 2 weeks (arrows in Figure 5D). At 3 months, a reduction in cell density of DRG neurons was evident (circle in Figure 5E), with improvement at 6 months (Figure 5F). Accompanying severe fiber degeneration and overall fiber loss were evident at 2weeks in sciatic nerve (arrows and circle respectively in Figure 5J) with less apparent sciatic nerve degeneration at 3months (Figure 5K). Further improvement was also observed in sciatic nerve at 6 months (Figure 5L). Morphometric analyses showed evidence of neuronal hypotrophy at 2 weeks, with nucleolar reduction in size evident and worsening at 3 months, but partially recovering at 6 months (Figure 5M). DRG and sciatic nerves from mice receiving IXA treatment also displayed moderate dark inclusions and mild fiber degeneration at 2 weeks post dose (respectively Supplementary Figures 2S and 3S, D) with recovery evident at later time points). G-ratio, the ratio between the axonal diameter/myelinated fibre diameter, was used as a measure of myelination and axonal integrity. Morphometric analyses showed neuronal hypotrophy with IXA at 2 weeks, similar to PACLI, whereas nucleolar reduction in size resolved at 3 months (unlike following PACLI), along with somatic recovery at 6 months (Supplementary Figure 4S, A–D). In contrast, DRG and sciatic nerves from ERIB and VINO treated mice showed no evidence of significant pathological change (see Figures 2S and 3S, A to L). Sciatic nerve morphometric evaluation showed decreased g-ratios at all time points for ERIB treated mice, and at 2 weeks and 3 months for VINO treated mice (V. Carozzi; personal communication).

Two weeks after cessation of dosing, only PACLI (Figure 5N) induced a moderate, but significant ($p < 0.01$), shift to the left of the G-ratio frequency distribution, indicating the occurrence of axonopathy. At 3 months following the cessation of dosing, this significant shift to the left of the distribution was still evident in the sciatic nerves of PACLI (Figure 5O), but there were no differences at the 6 month time point (Figure 5P).

Sciatic Nerve Immunofluorescence

To provide a cellular and molecular basis for the electrophysiological studies described above, we next quantified the neurodegenerative effects of each chemotherapy agent on axon area density, frequency of myelin abnormalities, abundance of non-neuronal nuclei, and tubulin biochemistry in cross-sections of sciatic nerves from drug and vehicle treated mice. Evidence of myelin abnormalities (Figure 6A (MBP), and 6B), likely secondary to axonopathy, was prominent at 2 weeks and 3 months and was consistently most frequent in PACLI-treated animals. In PACLI treated mice, axon area density was significantly decreased through 3 months of recovery (Figures 6A (PNF), 6C). In contrast, axon area density in ERIB treated mice recovered fully from initial deficits by the 2 week time point, with IXA and VINO showing no change at any time point. Only PACLI-treated mice displayed a significant and persistent increase in the number of non-neuronal nuclei at the 2

week, 3 month and 6 month recovery time points (Figure 6A (DAPI), 6D), although IXA treated mice showed a similar trend at 2 weeks (B. Cook; personal communication). These additional nuclei were positive for known Schwann cell markers S100B and GFAP, indicating that they are likely Schwann cells, the resident glia of the sciatic nerve (B.Cook; personal communication). Our previous work demonstrated that axonal levels of acetylated-α-tubulin, a marker of microtubule stability, were induced 11.7- and 4.6-fold for ERIB and PACLI-treated mice, respectively, at the end of a two week MTD treatment [26]. Here, we show that two weeks into the recovery phase, tubulin acetylation in ERIB treated mice is back to control levels while it was greatly reduced, but still significantly higher than vehicle treated mice, in PACLI treated mice (Figures 6A(Ac-tub), 6E). In contrast, axonal levels of both α-tubulin and end-binding protein 1 (EB1) rapidly returned to control values at 14 day from initially induced levels at the end of the MTD treatment in both PACLI and ERIB treated mice (B.Cook; personal communication). Overall, mice treated with ERIB-, IXA- and VINO recovered more rapidly from drug-induced morphological and biochemical effects than did PACLI-treated mice.

DISCUSSION

Previous investigations of chemotherapy-induced neurotoxicity have tended to focus on either pain behaviors or acute changes in nerve conduction velocity and amplitude. To our knowledge, there have been no systematic studies characterizing the time course of structural nerve and DRG injury and the completeness of recovery after exposure to neurotoxic chemotherapy. Understanding the underlying nature of DRG and peripheral nerve damage and recovery has become increasingly important as patients live longer with cancer, often receiving multiple, sequential courses of treatment with multiple neurotoxic agents, alone or in combination.

For these reasons, we have undertaken a longitudinal comparison of chemotherapy-induced peripheral neurotoxicity recovery in an animal model studying multiple independent endpoints. Four representative drugs that produce cytotoxic effects by interfering with microtubule function, including ERIB, IXA, PACLI and VINO, were investigated using an MTD dosing paradigm. The MTD doses used in these mice provided drug plasma exposures relatively similar and in the same rank order to the plasma exposures observed when therapeutic doses were administered to patients. The mouse plasma exposures for the four compounds also showed a similar rank order potency to their respective GI50 values reported against various human cancer cell lines, although there was much variability in these latter values (see Supplementary Table 1). All four drugs caused loss of intra-epidermal nerve fibers during the first two weeks after drug administration, which was determined to be the most sensitive measure of neurotoxic effects. Nerve conduction velocity and amplitude were most severely affected by PACLI and, to a lesser extent, IXA, and these effects were correlated with signs of degeneration in DRG and SN. The delayed recovery after PACLI was unique among the drugs studied, resulting in a severe, pervasive, and prolonged neuropathy consistent with more severe axonopathy. Compared to other agents studied, PACLI produced prolonged drug retention in sciatic nerve and DRG. For the other three microtubule targeting agents, injury was fully reversible after recovery of 3 to 6

months. These results may provide insight into the nature of clinically observed CIPN, including symptoms, relative severity and time course of recovery.

To our knowledge, this is the first comparative study of intra-epidermal nerve fiber loss and recovery in animal CIPN models. Previously, acute reductions in fiber density have been reported after PACLI or cisplatin (20). In addition, previous clinical studies have shown the usefulness of this measure in patient populations with small fiber neuropathy (30–33) or specifically after administration of IXA (34) and oxaliplatin (35). In the current study, the technique proved to be the most sensitive marker of distal small fiber injury during the first two weeks after drug administration with recovery in all cases. However, consistent with its more severe electrophysiological effects, PACLI caused the greatest loss and showed the slowest recovery. NCV reduction is consistent with myelin disruption in sciatic nerve. This effect was observed by immunohistochemistry at two weeks for all four agents, but the effect of PACLI was comparatively greater and more prolonged. Our experimental data are in agreement with clinical observations of neuropathy caused by all four drugs in both small fiber and large fiber sensory function, but the current observations suggest that the effects of PACLI are uniquely more severe. It would be of great interest to systematically evaluate changes in patients receiving chemotherapy to determine whether the time course of loss and recovery is similar to that observed here and establish the relationship between symptoms and intradermal fiber loss.

NCV and amplitude decreases after microtubule targeted chemotherapeutic agents have been previously reported (14,15,21,26,36–40). In the current study, PACLI and IXA produce the most severe acute deficits with ERIB and VINO causing milder effects. We previously followed animals for up to 28 days after dosing and observed similar patterns (21), with greater recovery in nerve conduction velocity compared to amplitude. It is notable, however, that ERIB treatment led to a delayed decrease in caudal amplitude that became significant only after 2 months of recovery. This pattern is similar to that observed previously (14,15), contrasting with the acute effects of PACLI and IXA and thus may be worthy of future investigation as to mechanism.

The morphological and biochemical assessments of acute cellular injury demonstrate a uniquely severe effect of PACLI, with axonal degeneration, DRG loss, alteration in G ratio and increase in Schwann cells observed most frequently after PACLI exposure. PACLI's induction of Schwann cells at all time points during the recovery phase is consistent with the notion that it generates the most cellular damage. IXA, which also has notable electrophysiological effects, also produced some signs of structural change, but the effects were in general milder than those caused by PACLI and recovery was more rapid. In general, ERIB caused few, if any, degenerative effects, other than early signs of myelin structure disruption. We previously reported that eribulin induces surprisingly favorable effects in microtubule biochemistry 24 h after MTD dosing which included increased axonal α-tubulin, acetylated tubulin, and EB1 [26]. These changes may promote a more stable cytoskeleton that allows eribulin-treated nerves to recover more quickly from its initial morphological effects. Surprisingly, VINO treatment was not associated with any significant degenerative effects in the sciatic nerve despite reductions in footpad IENFD, suggesting that different chemotherapies possess unique mechanisms of neuropathological induction.

Our data confirm that microtubule-targeting drugs induce axonopathy, but also suggest secondary myelin changes. After the MTD course administered in these experiments, these effects peak at about two weeks and are largely reversible. Neurotoxicity is more dramatic after PACLI and to a lesser extent after IXA. These effects may take longer to recover and in some cases were still present after even six months of recovery.

Even though all four chemotherapies rapidly cleared from plasma, each exhibited a prolonged exposure in DRG or sciatic nerve for 7 to 14 days, a phenomenon that may be associated with target binding and selective neurotoxicity. The unique effects of PACLI may be associated with its persistent residence in the nerve. As we have previously reported, while the drug is rapidly cleared from the circulation, PACLI was detectable in DRG and sciatic nerve through the final measurement at 60 days. While the absolute amount falls over time, the residual drug is likely tightly bound to microtubules causing persistent disruption of function and delaying recovery.

Persistent neuropathy after PACLI is a well-established clinical phenomenon in breast cancer survivors (41). Newer agents, like the ones studied here, have been developed and their cancer treatment trials have included assessment of neuropathy to establish comparative safety profiles (42–44). However, these clinical comparisons are difficult to interpret as they use subjective measures, and often involve second line therapy in patients previously exposed to neurotoxic chemotherapy including not only taxanes, but also platinum agents which also produce neuropathy. The difficulty of clinical comparisons is compounded by alterations in dosage size or frequencies that are often used to avoid the most severe neuropathy during the clinical trials. There is no long-term follow-up data regarding these newer agents as there is with the more commonly used agents like PACLI and cisplatin (3,41,45).

Thus, we believe that an important perspective is provided by the longitudinal animal data reported here, focusing on not only electrophysiology but also morphological, biochemical, IENFDs and drug levels in nerve and DRG. This data is at comparable dosing levels (MTD) and identical duration with recovery data uncomplicated by multiple treatment cycles used in the clinical setting (46). Interestingly, IENFDs is the most sensitive measure of neuropathy, showing acute changes for all the drugs studies. The acute axonopathy caused by microtubule disruption is also sensitively reflected in immunohistochemical disruption of myelin structure in the two weeks after administration for all drugs. There is no reason to believe there is a direct effect on myelin, but this observation suggests a close relationship between axons and Schwann cells. Our results further demonstrate that PACLI is a unique agent in its severity and lack of recovery associated with a prolonged residence of measureable drug in DRG and nerves. It produces larger, sometimes permanent effects on NCV and amplitude accompanied by morphological and biochemical evidence of degeneration in DRGs and sciatic nerve. IXA produces some of the same degenerative changes, but these are less prominent and more reversible. These data suggest that additional clinical studies should be undertaken to confirm the differences between agents to guide clinical practice.

Supplementary Material

Refer to Web version on PubMed Central for supplementary material.

Acknowledgments

Financial support: These studies were funded by a research support agreement from Eisai Inc. and an NIH grant R01CA161056 (to BSS) and utilized a NRI-MCDB Microscopy Facility at University of California, Santa Barbara supported by NIH S10OD010610.

References

1. Argyriou AA, Kyritsis AP, Makatsoris T, Kalofonos HP. Chemotherapy-induced peripheral neuropathy in adults: a comprehensive update of the literature. Cancer Manag Res. 2014; 6:135–47. [PubMed: 24672257]
2. Carlson K, Ocean AJ. Peripheral neuropathy with microtubule-targeting agents: occurrence and management approach. Clin Breast Cancer. 2011; 11(2):73–81. [PubMed: 21569993]
3. Windebank AJ, Grisold W. Chemotherapy-induced neuropathy. J Peripher Nerv Syst. 2008; 13(1): 27–46. [PubMed: 18346229]
4. Grisold W, Cavaletti G, Windebank AJ. Peripheral neuropathies from chemotherapeutics and targeted agents: diagnosis, treatment, and prevention. Neuro Oncol. 2012; 14(Suppl 4):iv45–54. [PubMed: 23095830]
5. Bhatnagar B, Gilmore S, Goloubeva O, Pelser C, Medeiros M, Chumsri S, et al. Chemotherapy dose reduction due to chemotherapy induced peripheral neuropathy in breast cancer patients receiving chemotherapy in the neoadjuvant or adjuvant settings: a single-center experience. Springerplus. 2014; 3:366. [PubMed: 25089251]
6. Fehrenbacher JC. Chemotherapy-induced peripheral neuropathy. Prog Mol Biol Transl Sci. 2015; 131:471–508. [PubMed: 25744683]
7. Griffith KA, Merkies IS, Hill EE, Cornblath DR. Measures of chemotherapy-induced peripheral neuropathy: a systematic review of psychometric properties. J Peripher Nerv Syst. 2010; 15(4):314–25. [PubMed: 21199103]
8. Boyette-Davis JA, Cata JP, Driver LC, Novy DM, Bruel BM, Mooring DL, et al. Persistent chemoneuropathy in patients receiving the plant alkaloids paclitaxel and vincristine. Cancer Chemother Pharmacol. 2013; 71(3):619–26. [PubMed: 23228992]
9. Quasthoff S, Hartung HP. Chemotherapy-induced peripheral neuropathy. J Neurol. 2002; 249(1):9–17. [PubMed: 11954874]
10. Han Y, Smith MT. Pathobiology of cancer chemotherapy-induced peripheral neuropathy (CIPN). Front Pharmacol. 2013; 4:156. [PubMed: 24385965]
11. Balayssac D, Ferrier J, Descoeur J, Ling B, Pezet D, Eschalier A, et al. Chemotherapy-induced peripheral neuropathies: from clinical relevance to preclinical evidence. Expert Opin Drug Saf. 2011; 10(3):407–17. [PubMed: 21210753]
12. Ocean AJ, Vahdat LT. Chemotherapy-induced peripheral neuropathy: pathogenesis and emerging therapies. Support Care Cancer. 2004; 12(9):619–25. [PubMed: 15258838]
13. Brell JM. Animal models of peripheral neuropathy: modeling what we feel, understanding what they feel. Ilar J. 2014; 54(3):253–8. [PubMed: 24615438]
14. Wozniak KM, Nomoto K, Lapidus RG, Wu Y, Carozzi V, Cavaletti G, et al. Comparison of neuropathy-inducing effects of eribulin mesylate, paclitaxel, and ixabepilone in mice. Cancer Res. 2011; 71(11):3952–62. [PubMed: 21498637]
15. Wozniak KM, Vornov JJ, Wu Y, Nomoto K, Littlefield BA, DesJardins C, et al. Sustained Accumulation of Microtubule-Binding Chemotherapy Drugs in the Peripheral Nervous System: Correlations with Time Course and Neurotoxic Severity. Cancer Res. 2016; 76(11):3332–9. [PubMed: 27197173]
16. Sahenk Z, Barohn R, New P, Mendell JR. Taxol neuropathy. Electrodiagnostic and sural nerve biopsy findings. Arch Neurol. 1994; 51(7):726–9. [PubMed: 7912506]

17. Xiao WH, Zheng H, Zheng FY, Nuydens R, Meert TF, Bennett GJ. Mitochondrial abnormality in sensory, but not motor, axons in paclitaxel-evoked painful peripheral neuropathy in the rat. Neuroscience. 2011; 199:461–9. [PubMed: 22037390]
18. Zheng H, Xiao WH, Bennett GJ. Mitotoxicity and bortezomib-induced chronic painful peripheral neuropathy. Exp Neurol. 2012; 238(2):225–34. [PubMed: 22947198]
19. Boyette-Davis J, Xin W, Zhang H, Dougherty PM. Intraepidermal nerve fiber loss corresponds to the development of taxol-induced hyperalgesia and can be prevented by treatment with minocycline. Pain. 2011; 152(2):308–13. [PubMed: 21145656]
20. Siau C, Xiao W, Bennett GJ. Paclitaxel- and vincristine-evoked painful peripheral neuropathies: loss of epidermal innervation and activation of Langerhans cells. Exp Neurol. 2006; 201(2):507–14. [PubMed: 16797537]
21. Wozniak KM, Wu Y, Farah MH, Littlefield BA, Nomoto K, Slusher BS. Neuropathy-inducing effects of eribulin mesylate versus paclitaxel in mice with preexisting neuropathy. Neurotox Res. 2013; 24(3):338–44. [PubMed: 23637052]
22. Liu Y, Sebastian B, Liu B, Zhang Y, Fissel JA, Pan B, et al. Sensory and autonomic function and structure in footpads of a diabetic mouse model. Sci Rep. 2017; 7:41401. [PubMed: 28128284]
23. Mortier KA, Renard V, Verstraete AG, Van Gussem A, Van Belle S, Lambert WE. Development and validation of a liquid chromatography-tandem mass spectrometry assay for the quantification of docetaxel and paclitaxel in human plasma and oral fluid. Anal Chem. 2005; 77(14):4677–83. [PubMed: 16013889]
24. Desjardins C, Saxton P, Lu SX, Li X, Rowbottom C, Wong YN. A high-performance liquid chromatography-tandem mass spectrometry method for the clinical combination study of carboplatin and anti-tumor agent eribulin mesylate (E7389) in human plasma. J Chromatogr B Analyt Technol Biomed Life Sci. 2008; 875(2):373–82.
25. Xu XS, Zeng J, Mylott W, Arnold M, Waltrip J, Iacono L, et al. Liquid chromatography and tandem mass spectrometry for the quantitative determination of ixabepilone (BMS-247550, Ixempra) in human plasma: method validation, overcoming curve splitting issues and eliminating chromatographic interferences from degradants. J Chromatogr B Analyt Technol Biomed Life Sci. 2010; 878(5–6):525–37.
26. Carozzi VA, Canta A, Oggioni N, Sala B, Chiorazzi A, Meregalli C, et al. Neurophysiological and neuropathological characterization of new murine models of chemotherapy-induced chronic peripheral neuropathies. Exp Neurol. 2010; 226(2):301–9. [PubMed: 20832406]
27. Cavaletti G, Tredici G, Marmiroli P, Petruccioli MG, Barajon I, Fabbrica D. Morphometric study of the sensory neuron and peripheral nerve changes induced by chronic cisplatin (DDP) administration in rats. Acta Neuropathol. 1992; 84(4):364–71. [PubMed: 1441917]
28. Carozzi VA, Chiorazzi A, Canta A, Meregalli C, Oggioni N, Cavaletti G, et al. Chemotherapy-induced peripheral neurotoxicity in immune-deficient mice: new useful ready-to-use animal models. Exp Neurol. 2015; 264:92–102. [PubMed: 25450467]
29. Benbow SJ, Cook BM, Reifert J, Wozniak KM, Slusher BS, Littlefield BA, et al. Effects of Paclitaxel and Eribulin in Mouse Sciatic Nerve: A Microtubule-Based Rationale for the Differential Induction of Chemotherapy-Induced Peripheral Neuropathy. Neurotox Res. 2015
30. Khoshnoodi MA, Ebenezer GJ, Polydefkis M. Epidermal innervation as a tool to study human axonal regeneration and disease progression. Exp Neurol. 2017; 287(Pt 3):358–64. [PubMed: 27317299]
31. Khoshnoodi MA, Truelove S, Burakgazi A, Hoke A, Mammen AL, Polydefkis M. Longitudinal Assessment of Small Fiber Neuropathy: Evidence of a Non-Length-Dependent Distal Axonopathy. JAMA Neurol. 2016; 73(6):684–90. [PubMed: 27065313]
32. Ebenezer GJ, Hauer P, Gibbons C, McArthur JC, Polydefkis M. Assessment of epidermal nerve fibers: a new diagnostic and predictive tool for peripheral neuropathies. J Neuropathol Exp Neurol. 2007; 66(12):1059–73. [PubMed: 18090915]
33. Ebenezer GJ, McArthur JC, Thomas D, Murinson B, Hauer P, Polydefkis M, et al. Denervation of skin in neuropathies: the sequence of axonal and Schwann cell changes in skin biopsies. Brain. 2007; 130(Pt 10):2703–14. [PubMed: 17898011]

34. Ebenezer GJ, Carlson K, Donovan D, Cobham M, Chuang E, Moore A, et al. Ixabepilone-induced mitochondria and sensory axon loss in breast cancer patients. Ann Clin Transl Neurol. 2014; 1(9): 639–49. [PubMed: 25493278]

35. Burakgazi AZ, Messersmith W, Vaidya D, Hauer P, Hoke A, Polydefkis M. Longitudinal assessment of oxaliplatin-induced neuropathy. Neurology. 2011; 77(10):980–6. [PubMed: 21865571]

36. Carozzi VA, Chiorazzi A, Canta A, Lapidus RG, Slusher BS, Wozniak KM, et al. Glutamate carboxypeptidase inhibition reduces the severity of chemotherapy-induced peripheral neurotoxicity in rat. Neurotox Res. 2010; 17(4):380–91. [PubMed: 19763734]

37. Carozzi V, Chiorazzi A, Canta A, Oggioni N, Gilardini A, Rodriguez-Menendez V, et al. Effect of the chronic combined administration of cisplatin and paclitaxel in a rat model of peripheral neurotoxicity. Eur J Cancer. 2009; 45(4):656–65. [PubMed: 19091544]

38. Boehmerle W, Huehnchen P, Peruzzaro S, Balkaya M, Endres M. Electrophysiological, behavioral and histological characterization of paclitaxel, cisplatin, vincristine and bortezomib-induced neuropathy in C57Bl/6 mice. Sci Rep. 2014; 4:6370. [PubMed: 25231679]

39. Leandri M, Ghignotti M, Emionite L, Leandri S, Cilli M. Electrophysiological features of the mouse tail nerves and their changes in chemotherapy induced peripheral neuropathy (CIPN). J Neurosci Methods. 2012; 209(2):403–9. [PubMed: 22800858]

40. Pisano C, Pratesi G, Laccabue D, Zunino F, Lo Giudice P, Bellucci A, et al. Paclitaxel and Cisplatin-induced neurotoxicity: a protective role of acetyl-L-carnitine. Clin Cancer Res. 2003; 9(15):5756–67. [PubMed: 14654561]

41. Hershman DL, Weimer LH, Wang A, Kranwinkel G, Brafman L, Fuentes D, et al. Association between patient reported outcomes and quantitative sensory tests for measuring long-term neurotoxicity in breast cancer survivors treated with adjuvant paclitaxel chemotherapy. Breast Cancer Res Treat. 2011; 125(3):767–74. [PubMed: 21128110]

42. Chang WJ, Sun JM, Lee JY, Ahn JS, Ahn MJ, Park K. A retrospective comparison of adjuvant chemotherapeutic regimens for non-small cell lung cancer (NSCLC): paclitaxel plus carboplatin versus vinorelbine plus cisplatin. Lung Cancer. 2014; 84(1):51–5. [PubMed: 24521819]

43. Kelly K, Crowley J, Bunn PA Jr, Presant CA, Grevstad PK, Moinpour CM, et al. Randomized phase III trial of paclitaxel plus carboplatin versus vinorelbine plus cisplatin in the treatment of patients with advanced non--small-cell lung cancer: a Southwest Oncology Group trial. J Clin Oncol. 2001; 19(13):3210–8. [PubMed: 11432888]

44. Vahdat LT, Garcia AA, Vogel C, Pellegrino C, Lindquist DL, Iannotti N, et al. Eribulin mesylate versus ixabepilone in patients with metastatic breast cancer: a randomized Phase II study comparing the incidence of peripheral neuropathy. Breast Cancer Res Treat. 2013; 140(2):341–51. [PubMed: 23877339]

45. Strumberg D, Brugge S, Korn MW, Koeppen S, Ranft J, Scheiber G, et al. Evaluation of long-term toxicity in patients after cisplatin-based chemotherapy for non-seminomatous testicular cancer. Annals of oncology : official journal of the European Society for Medical Oncology. 2002; 13(2): 229–36. [PubMed: 11885999]

46. Pace A, Nistico C, Cuppone F, Bria E, Galie E, Graziano G, et al. Peripheral neurotoxicity of weekly paclitaxel chemotherapy: a schedule or a dose issue? Clin Breast Cancer. 2007; 7(7):550–4. [PubMed: 17509163]

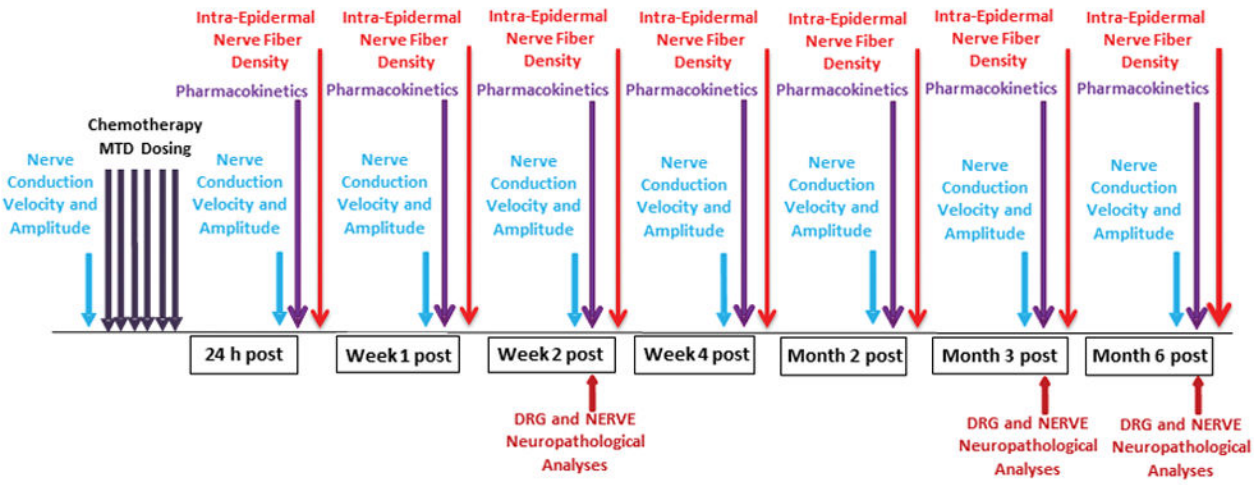

Figure 1.

Experimental schematic of mouse procedures and experimental endpoints. Mice were assessed for baseline nerve conduction velocity /amplitude (functional assessment) prior to the intravenous 6-dose MTD regimen and again at 24 h, 1 week, 2 weeks, 4 weeks, 2 months, 3 months and 6 months after dosing. At similar time points, foot pads, plasma, DRG and sciatic nerve samples were collected from mice for intra-epidermal nerve fiber density (IENFD) quantification and bioanalysis of drug levels (PK), respectively. In addition, DRG and sciatic nerve samples were collected for morphological/morphometric evaluations at the 2 week, 3 month and 6 month time points.

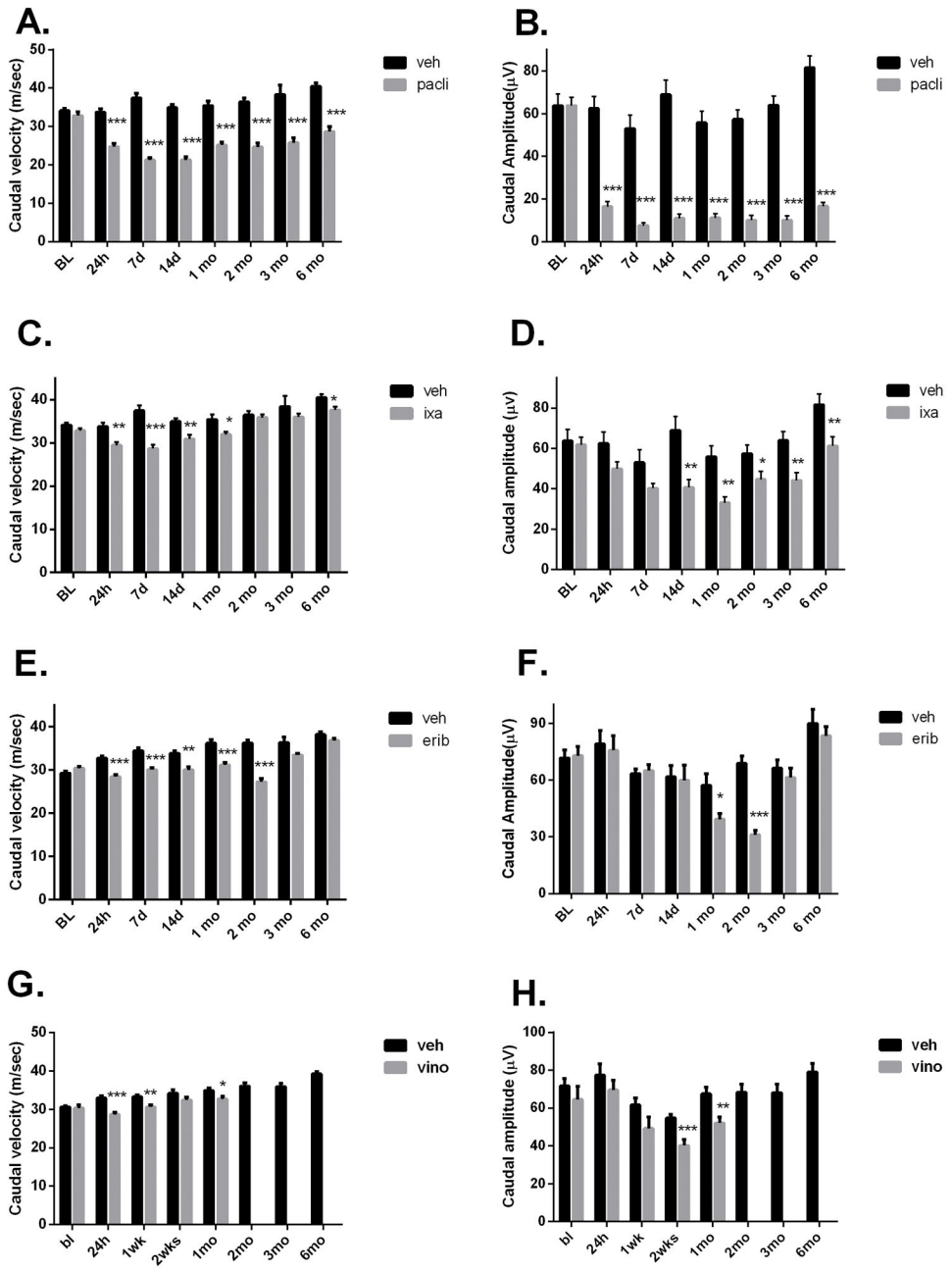

Figure 2.

Effect of MTD dosing on caudal nerve conduction and amplitude. Mice dosed with PACLI showed the most severe and longest lasting deficits in caudal velocity and amplitude, followed by IXA, ERIB and lastly VINO, which produced the least severe changes (Students t test: *p<0.05, **p<0.01, ***p<0.001 versus vehicle). N= 10 mice /group except for VINO where n= 8 mice/group.

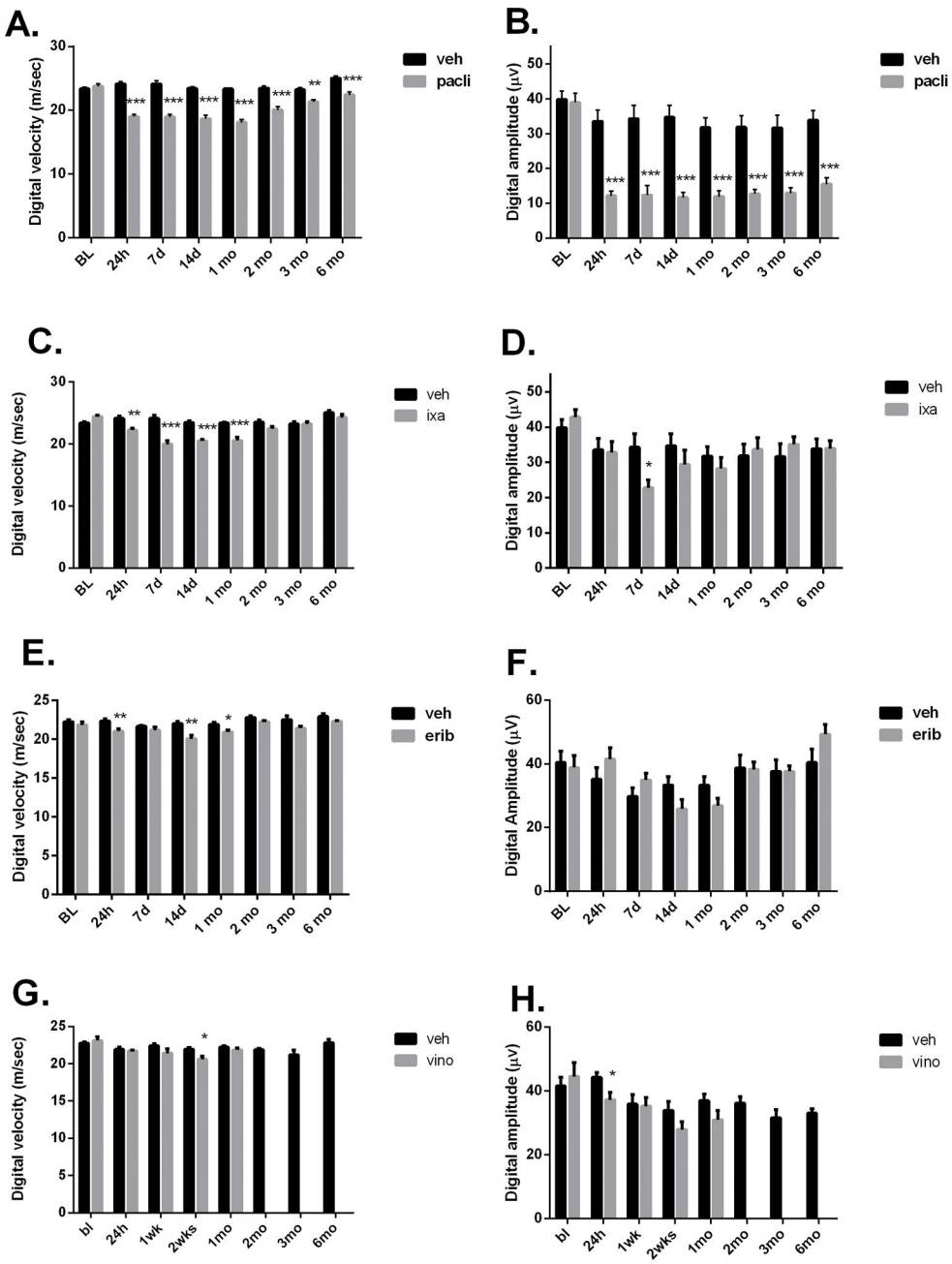

Figure 3.

Effect of MTD dosing on digital nerve conduction and amplitude in mice. Mice dosed with PACLI produced the most severe digital nerve conduction velocity and amplitude deficits, followed by IXA and then ERIB and VINO. Digital amplitude was not significantly affected by ERIB or VINO at any time point studied (Students-t test: *p<0.05, **p<0.01, ***p<0.001 versus vehicle). N= 10 mice /group except for VINO where n= 8 mice/group.

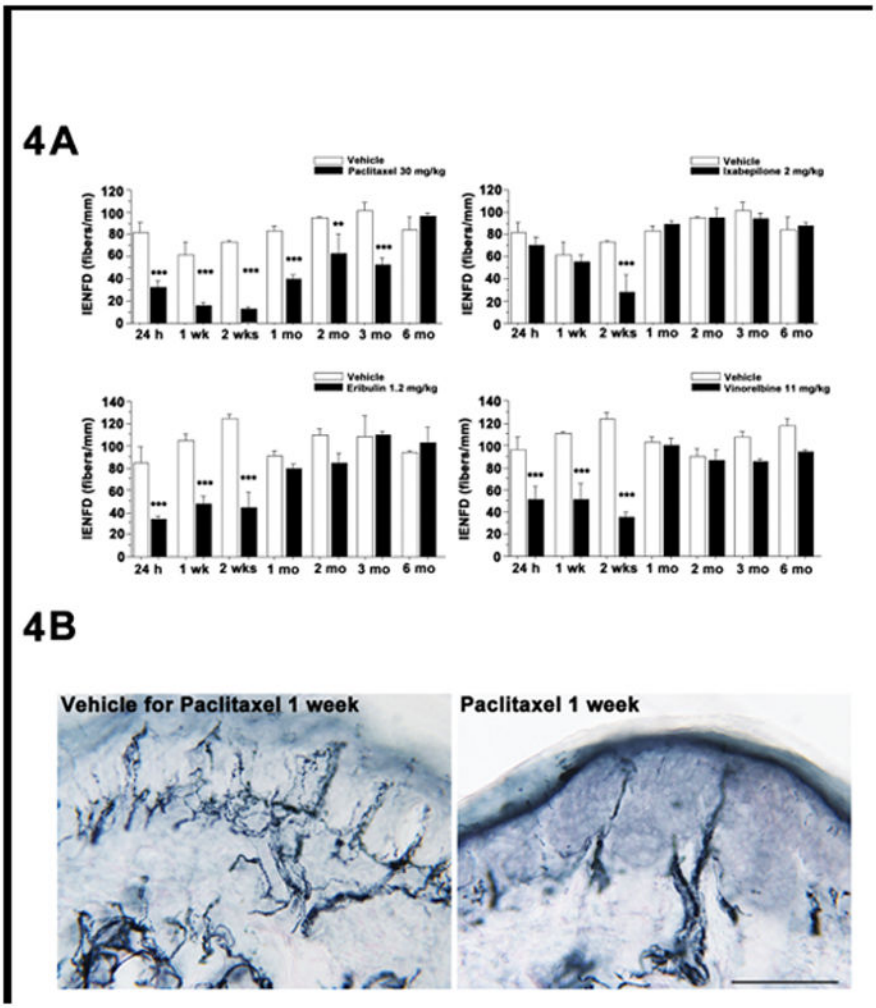

Figure 4.

Effect of MTD chemotherapy dosing on footpad intra-epidermal nerve fiber density (IENDF) in mice. A: PACLI induced a significant and sustained reduction in intra-epidermal nerve fiber density (PGP positive fibers) from 24 hours to 3 months after dosing. VINO and ERIB also produced deficits from 24h, but these recovered by 4 weeks and IXA treated mice showed a significant deficit in fiber density at 2 weeks and recovered thereafter. (Student's t test: ** $p < 0.01$, *** $p < 0.001$, versus vehicle-treated mice). B: Representative photomicrographs of PGP positive fibers indicating loss of intra-epidermal nerve fiber density in PACLI-treated mice 1 week after cessation of treatment versus vehicle. N=3 mice/timepoint/treatment.

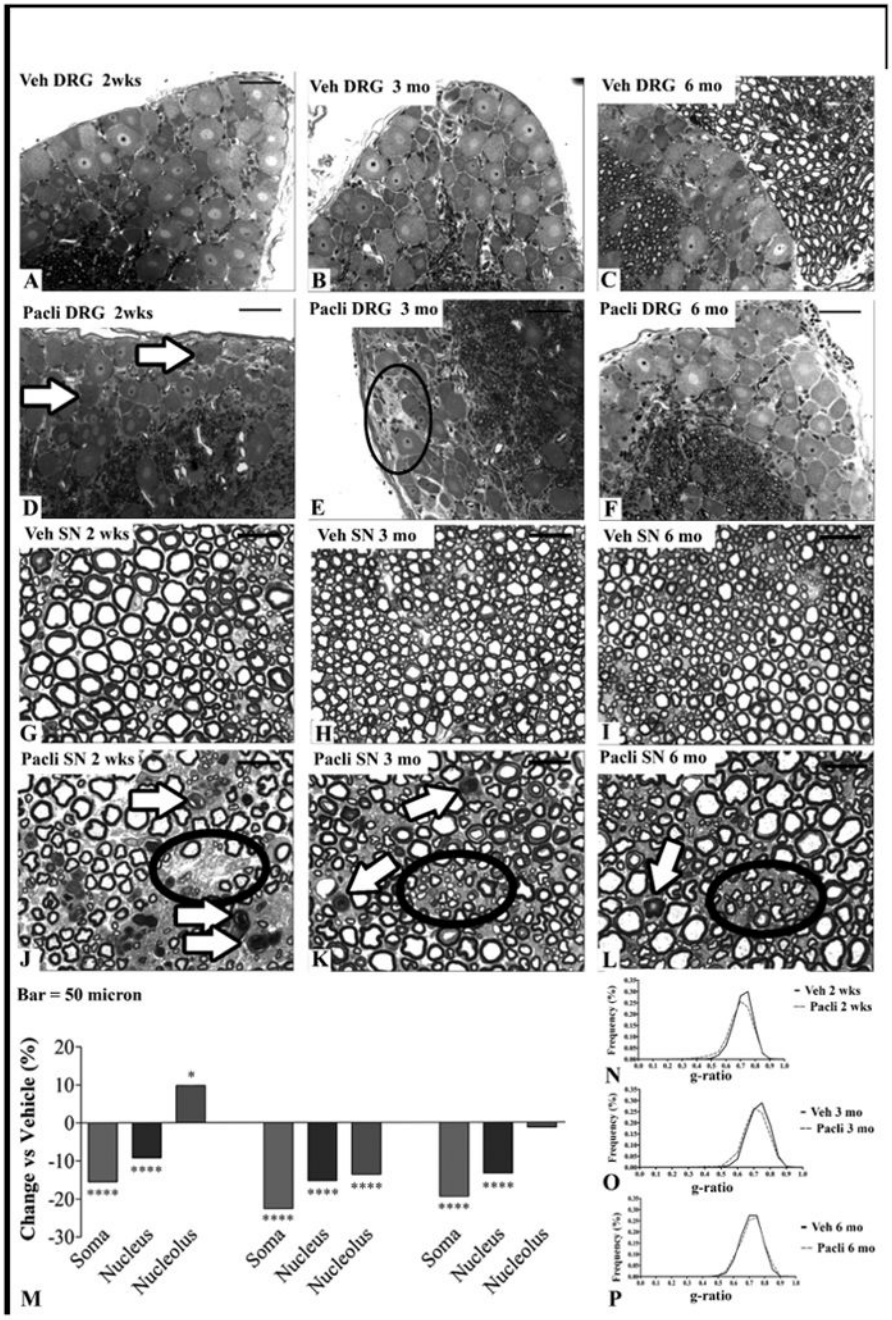

Figure 5.

(A–L): Light microscopy analysis of the sciatic nerve and DRG of vehicle and PACLI-treated mice. After 2 weeks of recovery, PACLI induced cytoplasmic dark spot inclusions, particularly frequent in large neurons (arrows in **D**). At 3 months, there was sporadic degeneration/loss of sensory neurons (circle on **E**) with general improvement after 6 months (**F**). At 2 weeks PACLI induced axonopathy (white arrows in **J**) and fiber loss (circle in **J**) was evident. Similar but milder damages persisted after 3 (K) and 6 months (L).

(M): Morphometric analysis of DRG sensory neurons and sciatic nerves of vehicle and

PACLI- treated mice shows the rate change (%) of DRG neuronal cellular sizes of PACLI versus vehicle-treated mice. PACLI induced a severe somatic (***p<0.0001 vs vehicle) and nuclear (***p<0.0001 vs vehicle) reduction-in-size at 2 weeks. The damage worsened at 3 months but partially recovered at 6 months. (***p<0.0001 versus vehicle; *p<0.05 vs vehicle: Student's t test). **(N–P):** G-ratio (estimated by dividing the axon diameter by the myelinated fibre diameter) was calculated as a measure of myelination and axonal integrity of sciatic nerves. The graphs in **N**, **O** and **P** depict the frequency distribution of myelinated fibres g-ratio (%) after 2 weeks, 3 months and 6 months, respectively. PACLI induced a significant (p<0.01) shift to the left of the histograms at 2 weeks, indicating a reduction in the frequency of the largest fibers **(N)** which was still present thru 3 months (**O**), but resolved after 6 months **(P).** N=3 mice/timepoint/treatment.

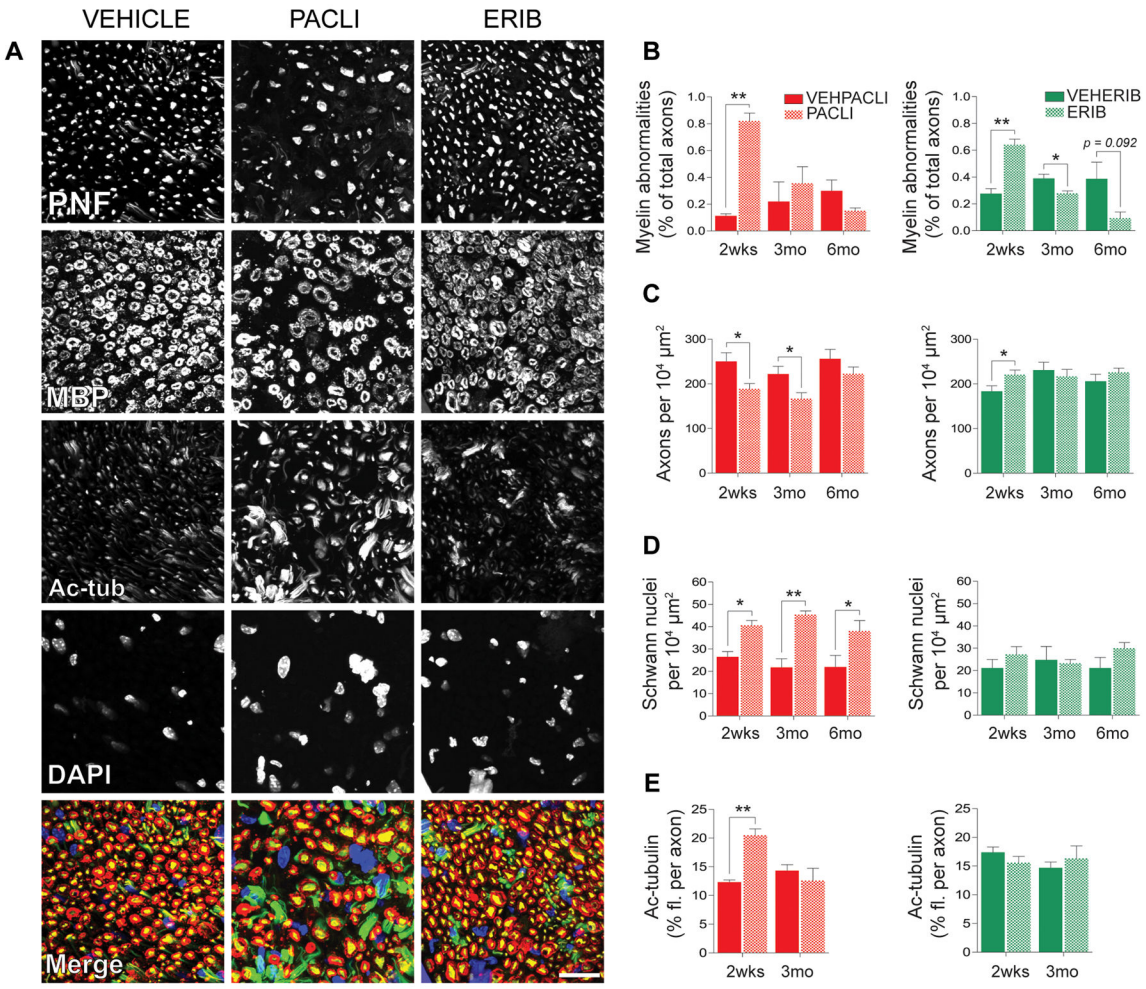

Figure 6.

Quantitative immunofluorescence analysis of sciatic nerve cross-sections. Mice dosed with PACLI produced the most severe effects on myelin, axon area density, and non-neuronal (Schwann) nuclei, followed by ERIB. IXA and VINO had no effect (data not shown). (A) representative images of drug and vehicle treated mice following a recovery period of two weeks. PNF = phosphoneurofilament (axons, yellow), MBP = myelin basic protein (myelin sheath, red), acetylated tubulin (K40Ac, green), DAPI (nuclei, blue), scale bar = 20µm. As there was no significant difference among the vehicles for PACLI/IXA, VINO, and ERIB by any measure, only the vehicle for PACLI/IXA is shown. Quantification of (B) frequency of myelin abnormalities from MBP, (C) axons per unit area from PNF, (D) number of non-neuronal (Schwann) nuclei per unit area from DAPI, and (E) quantification of relative axonal abundance of acetylated tubulin during the recovery period after mice receiving an MTD dosing regimen. Tubulin acetylation in ERIB treated mice returned to control levels while it was greatly reduced but still significantly higher than vehicle treated mice in PACLI treated mice. Student-t tests were used to identify significant differences between comparisons of the drug groups to their respective vehicles at each time point, *$p<0.05$, **$p<0.01$.

Table 1

Chemotherapy drug concentrations in plasma, DRG and sciatic nerve

	Treatment / Concentration (ng/g) or (ng/mL)											
Day	ERIB (1.2 mg/kg)			IXA (2 mg/kg)			PACLI (30 mg/kg)			VINO (11 mg/kg)		
	DRG	sciatic nerve	plasma #	DRG	sciatic nerve	plasma #	DRG	sciatic nerve	plasma #	DRG	sciatic nerve	plasma #
1	75.5	68.0	BLQ	549	BLQ	BLQ	6450	1550	4.68	1490	64.3	5.56
7	14.8	43.4	BLQ	205	BLQ	BLQ	615	629	BLQ	376	32.5	BLQ
14	BLQ	17.6	0.79 *	BLQ	BLQ	BLQ	412	703	BLQ	91.8	BLQ	BLQ
28	BLQ	BLQ	BLQ	BLQ	BLQ	BLQ	84.1	85.4	BLQ	BLQ	BLQ	BLQ
60	BLQ	BLQ	BLQ	BLQ	BLQ	BLQ	17.7	10.4	BLQ	BLQ	BLQ	BLQ

BLQ= below limit of quantification

mean of samples from 3 mice

* 2/3 samples BLQ